

## ELECTRONIC SUPPORTING INFORMATION

### Synthesis, structure and magnetic investigations of dinuclear lanthanide complexes based on 2-ethoxycinnamate..

Amina Zouzou<sup>a</sup> Adel Beghidja\*,<sup>a</sup> Jérôme Long\*,<sup>b</sup> Chahrazed Beghidja,<sup>a</sup> Felipe Gandara,<sup>c</sup> Yannick Guari<sup>b</sup> and Joulia Larionova<sup>b</sup>

a. Unité de Recherche de Chimie de l'Environnement et Moléculaire Structurale (CHEMS), Université frères Mentouri Constantine, Route Aïn elbey, 25000 Constantine, (Algérie). E-mail: a\_beghidja@yahoo.fr

b. Institut Charles Gerhardt Montpellier, UMR 5253, Ingénierie Moléculaire et Nano-Objets, Université de Montpellier, ENSCM, CNRS, Place E. Bataillon, 34095 Montpellier Cedex 5 (France). E-mail: jerome.long@umontpellier.fr

c. Departamento de Nuevas Arquitecturas en Química de Materiales, The Materials Science Factory, Instituto de Ciencia de Materiales de Madrid (ICMM-CSIC), Sor Juana Inés de la Cruz 3, Cantoblanco 28049, Madrid (Spain).

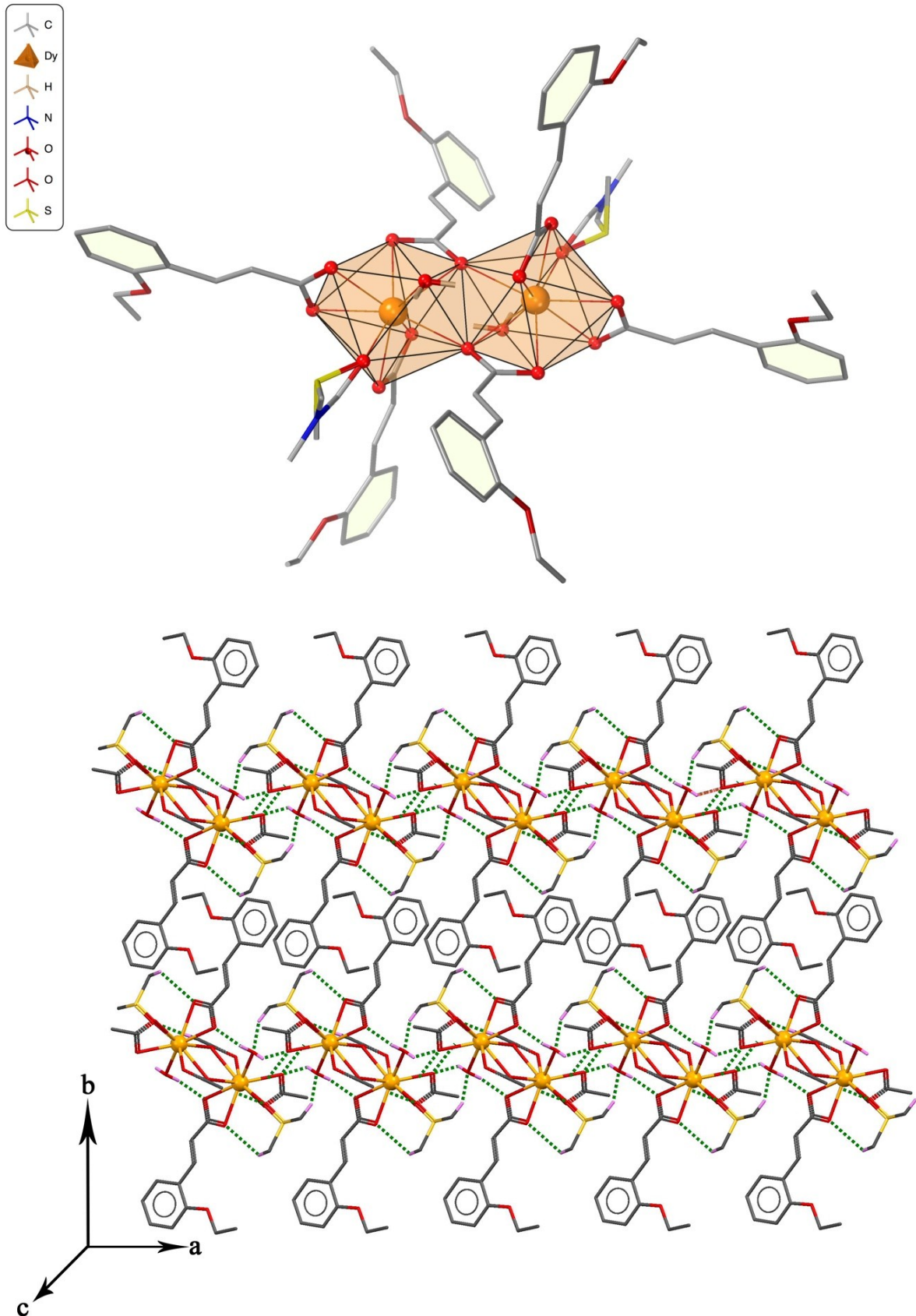


**Figure S1:** Top: Structure of the dinuclear complexes (**3**, **5**, **6**). Hydrogen atoms are omitted for clarity. Bottom: crystal packing.

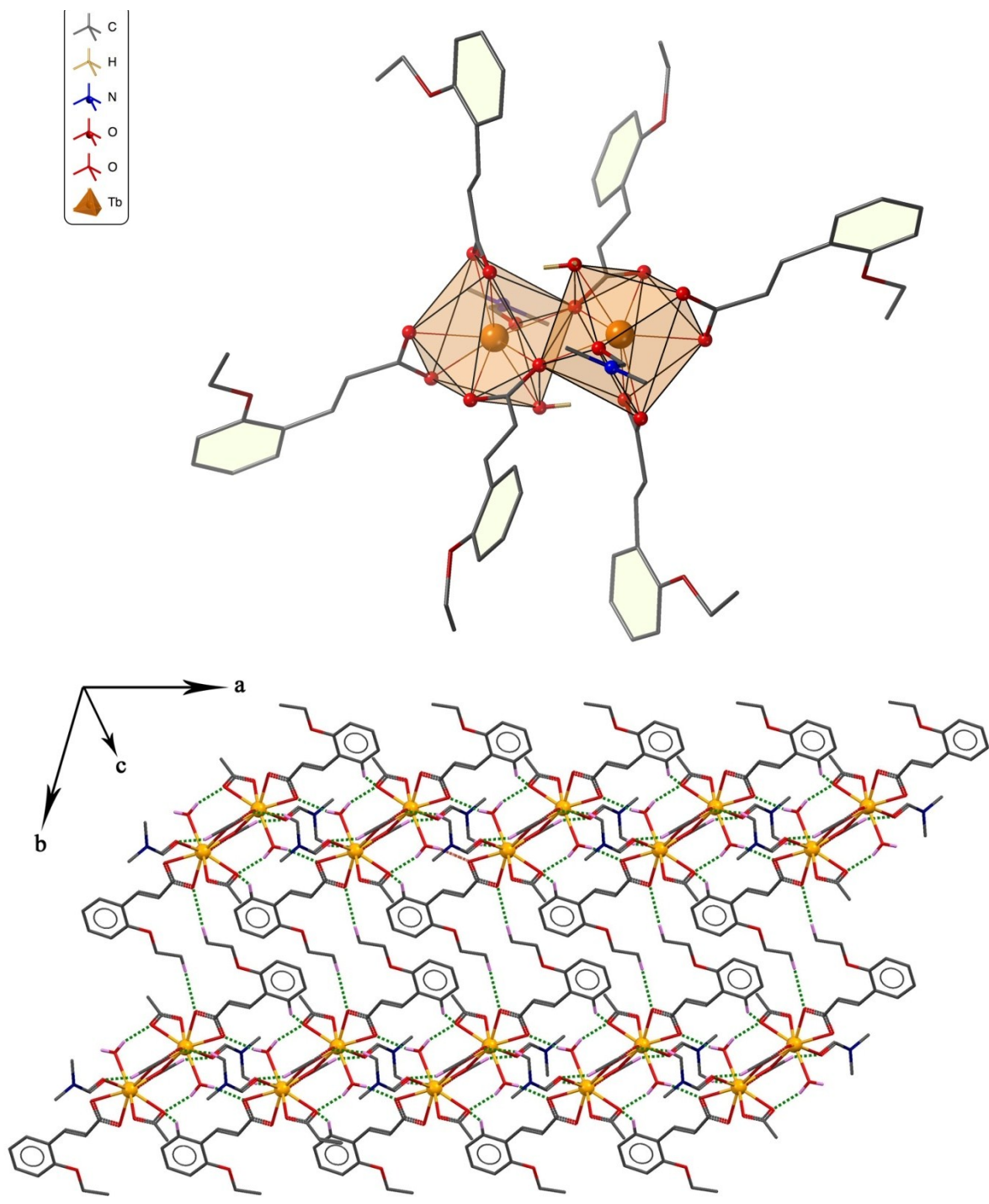


**Figure S2:** Top: Structure of the dinuclear complex 4. Hydrogen atoms are omitted for clarity.  
Bottom: crystal packing.

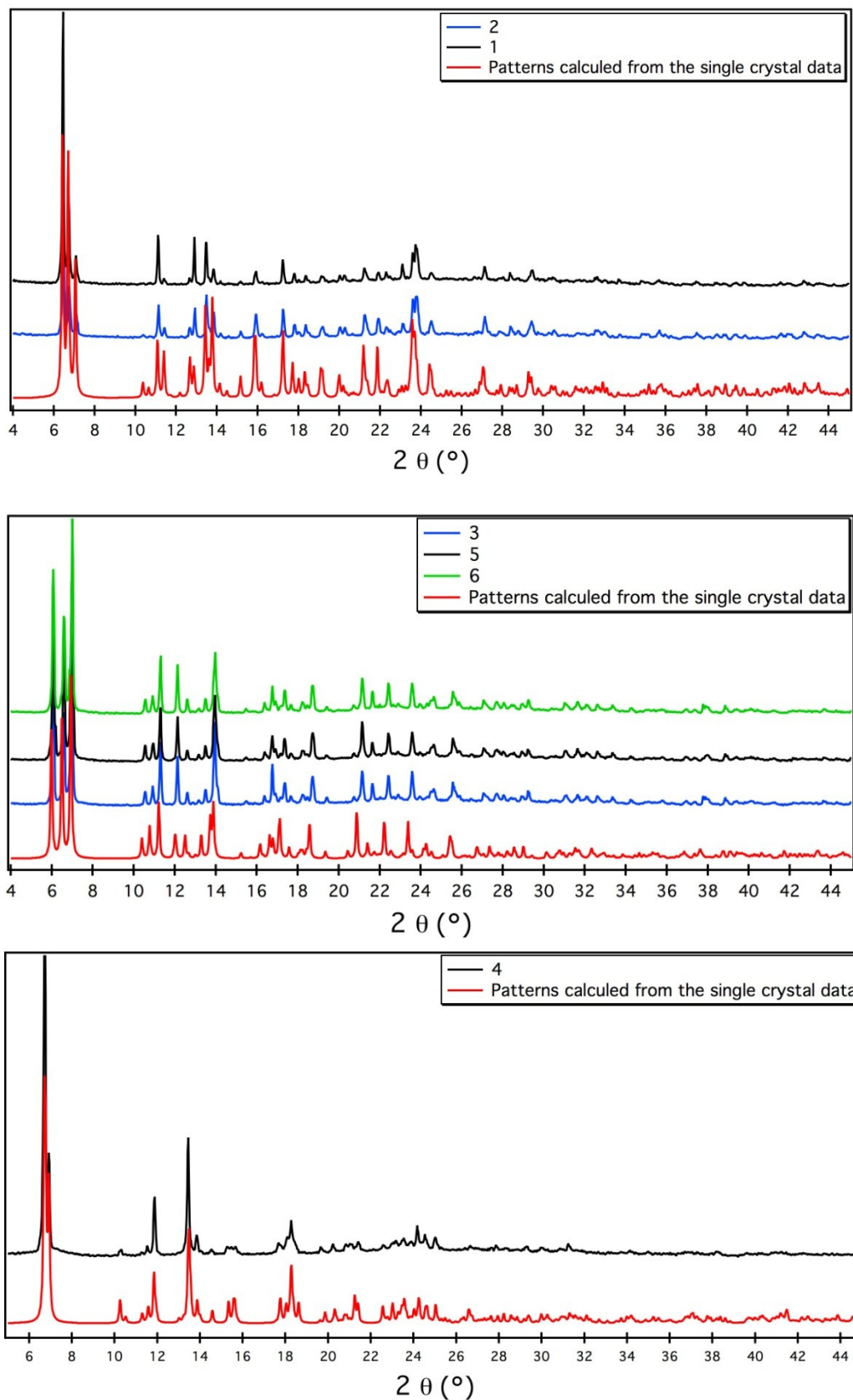


**Figure S3** Powder X-ray diffraction patterns (Cu K $\alpha$ 1) from experiment and simulated for **1-6**.

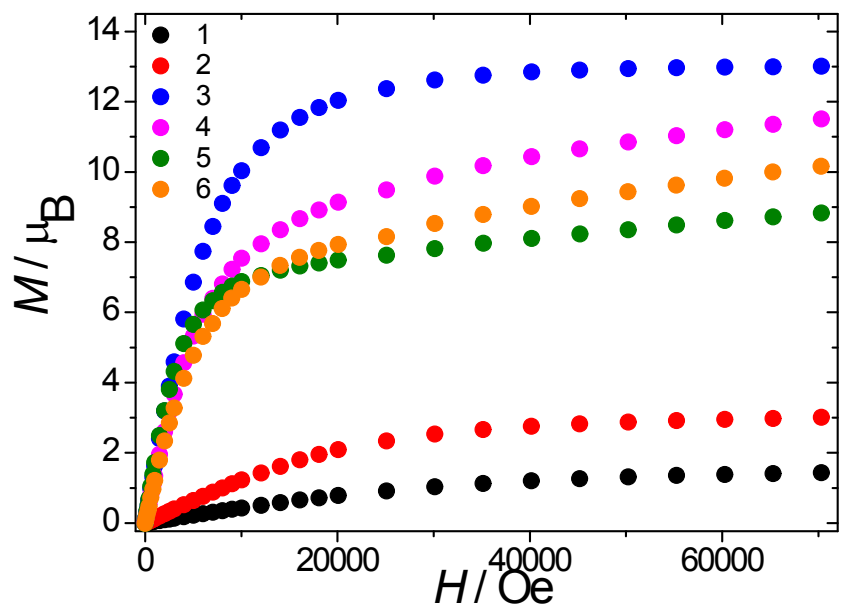


**Figure S4:** Field dependence of the magnetisation at 1.8 K for **1-6**.

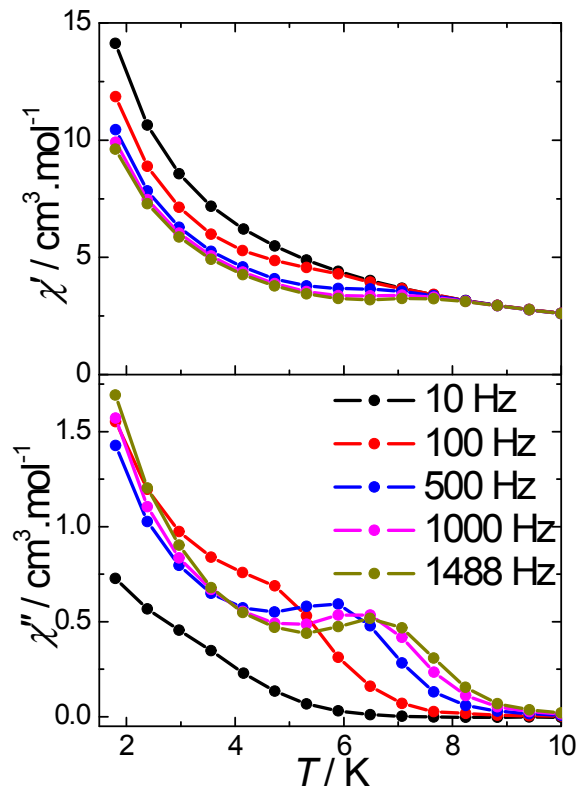


**Figure S5:** Temperature dependence of ac susceptibilities for **5** under a zero dc-field.

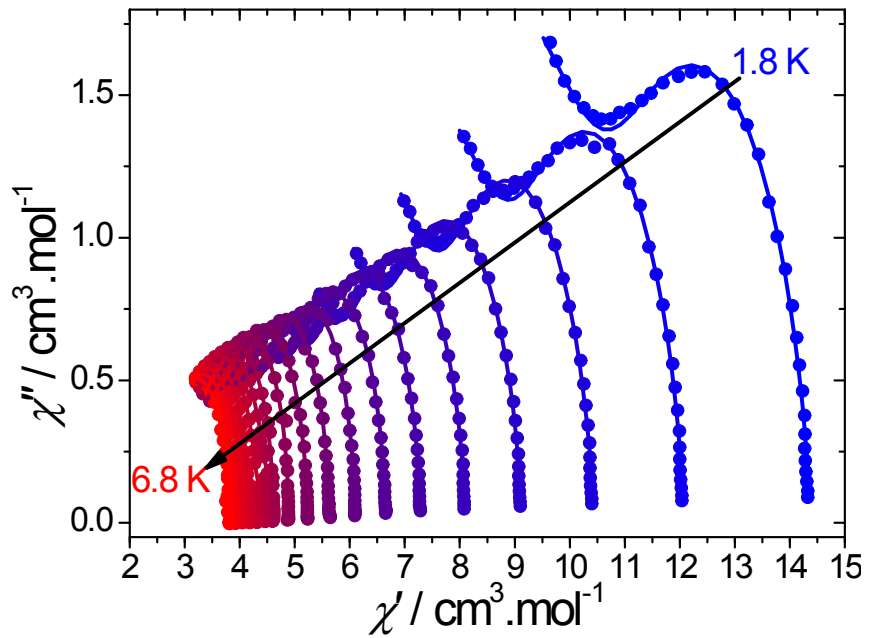


**Figure S6:** Cole-Cole plots using the ac data performed under a zero dc-field for **5**. The solid lines correspond to the fit with a sum of two Debye functions.<sup>1</sup>

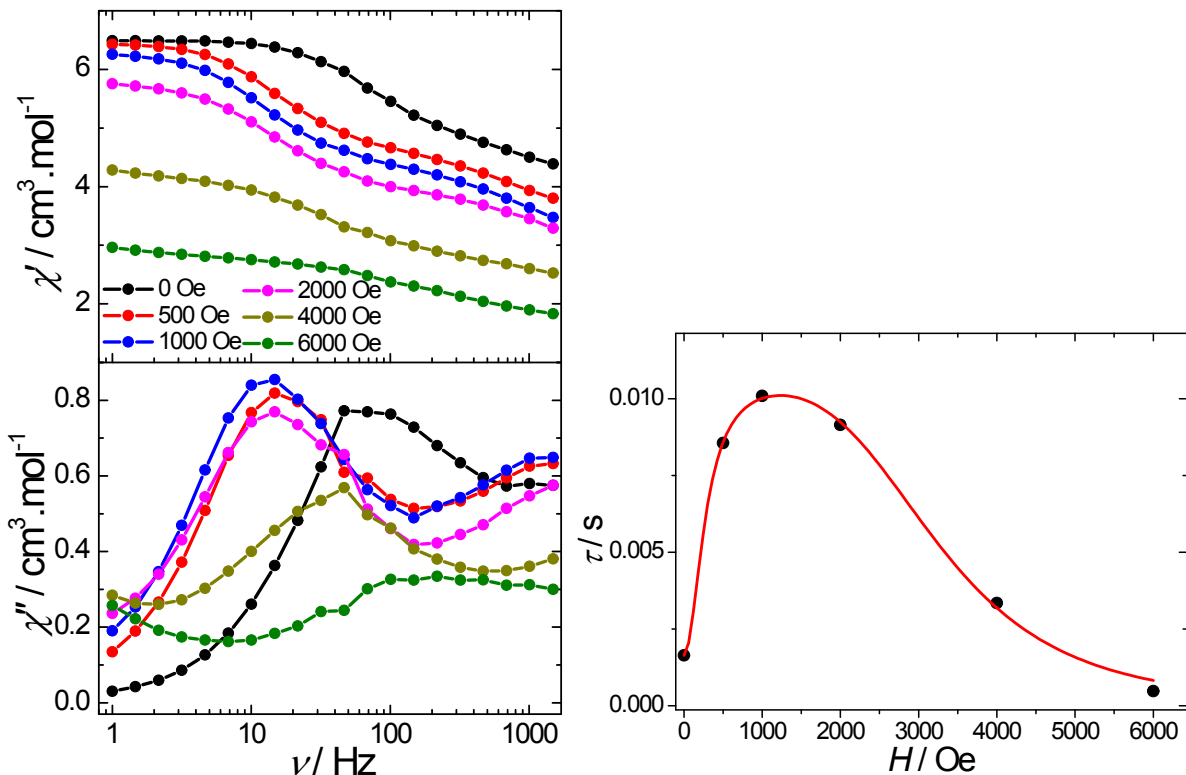


**Figure S7:** Left: frequency dependence of the ac susceptibilities at 4 K for **5** under various dc fields. Right: field dependence of the relaxation time at 4 K for **5**. The red solid line corresponds to the fit with Eq. 2.

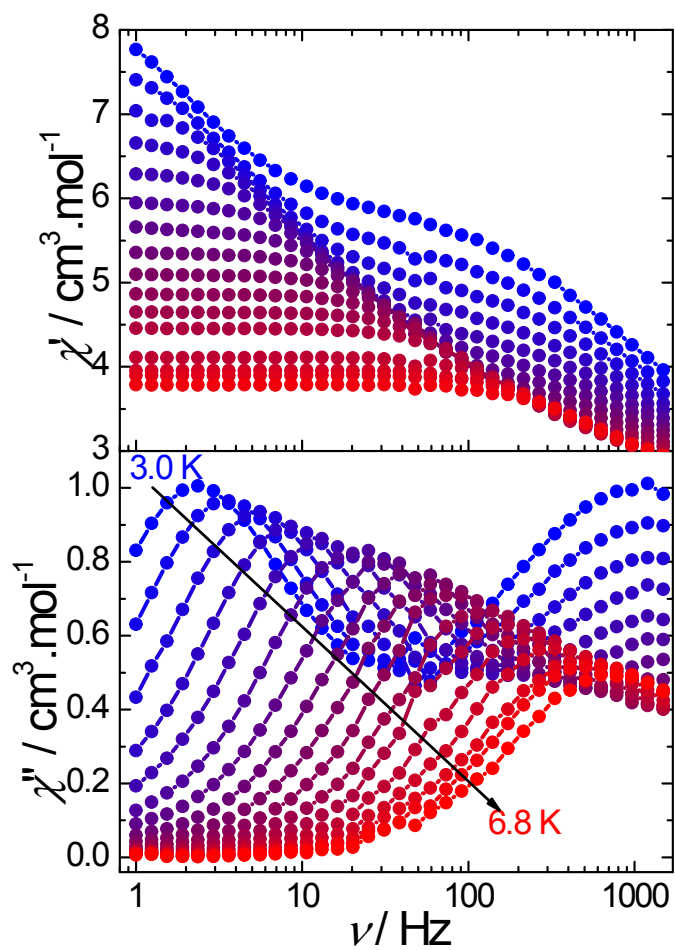


**Figure S8:** Frequency dependence of ac susceptibilities for **5** under a 1000 Oe field.

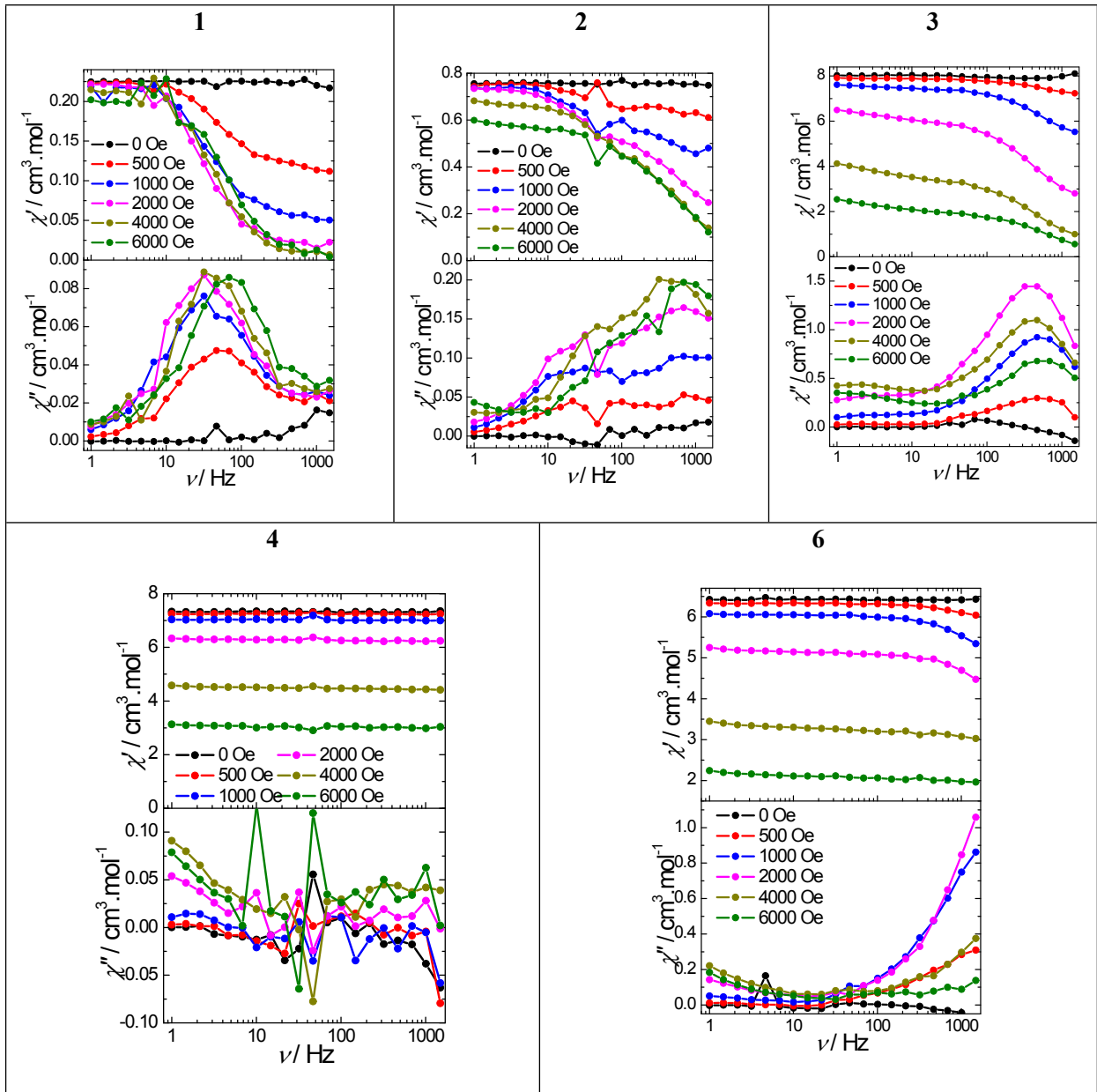


**Figure S9:** Frequency dependence of the ac susceptibilities at 2 K under various dc fields.

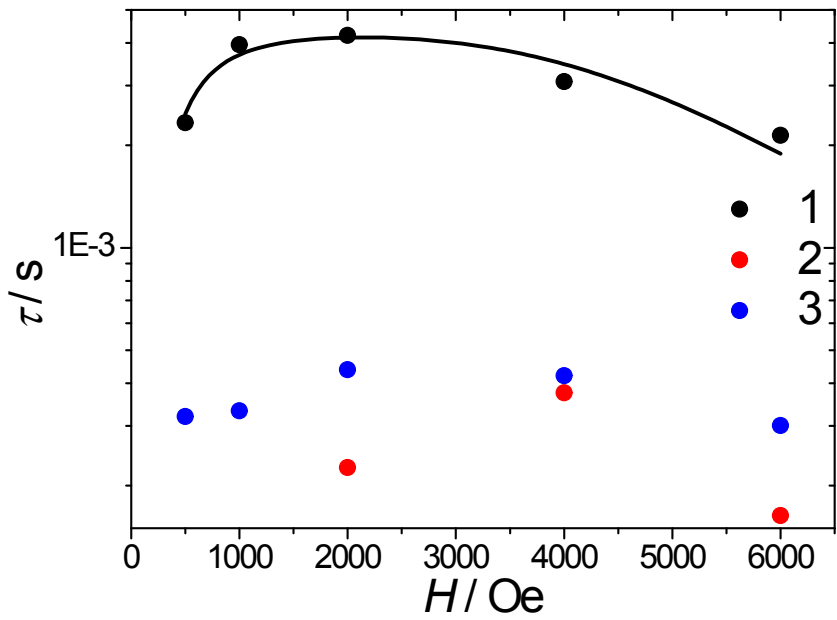


**Figure S10:** Field dependence of the relaxation time at 2 K for **1–3**. The solid line corresponds to the fit with Eq. 2.

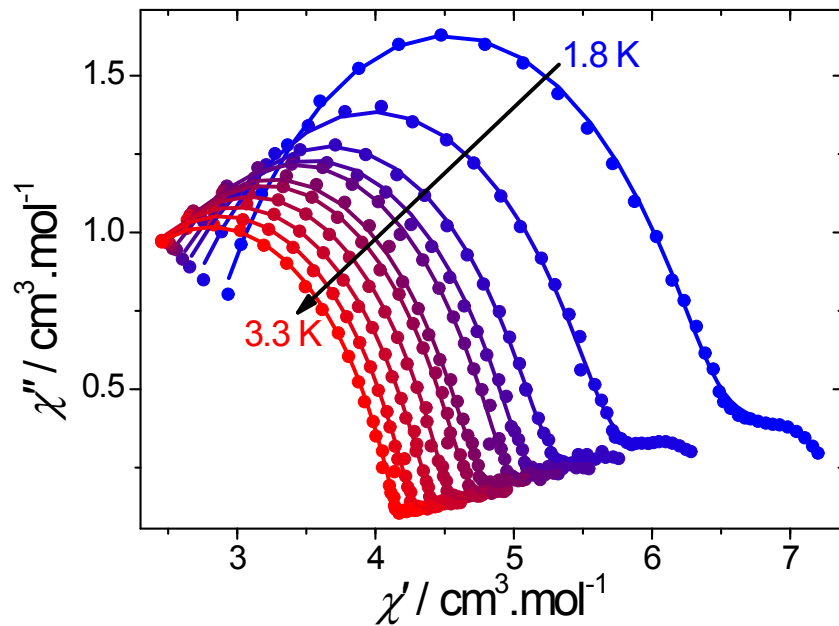


**Figure S11:** Cole-Cole plots using the ac data performed under a 2000 Oe dc-field for **3**. The solid lines correspond to the fit with a sum of two Debye functions.

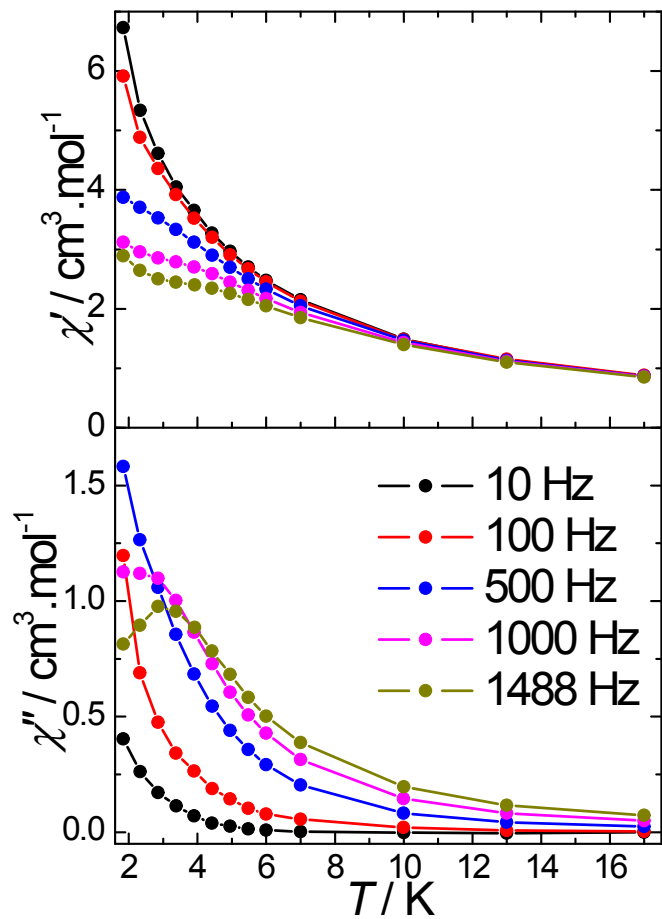


**Figure S12:** Temperature dependence of ac susceptibilities for **3** under a 2000 Oe dc-field.

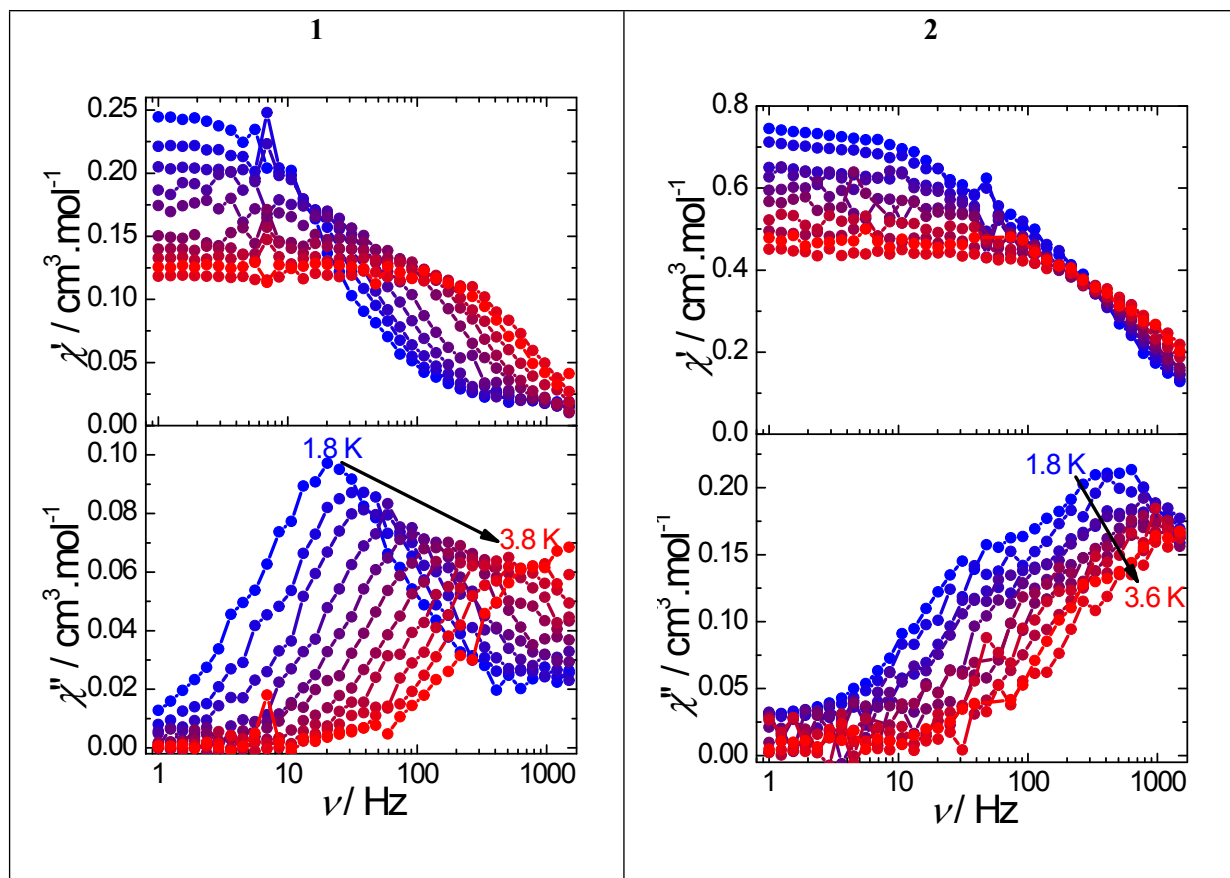


**Figure S13:** Frequency dependence of ac susceptibilities for **1** and **2** under a 2000 Oe and 4000 Oe dc field respectively.

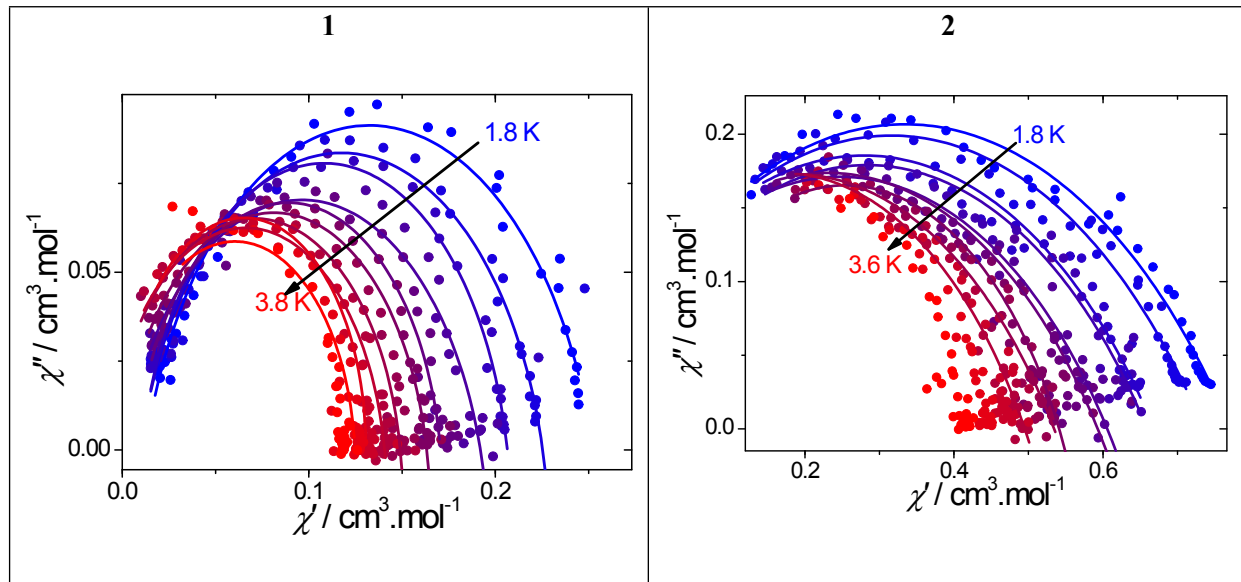


**Figure S14:** Frequency dependence of ac susceptibilities for **1** and **2** under a 2000 Oe and 4000 Oe dc field respectively.

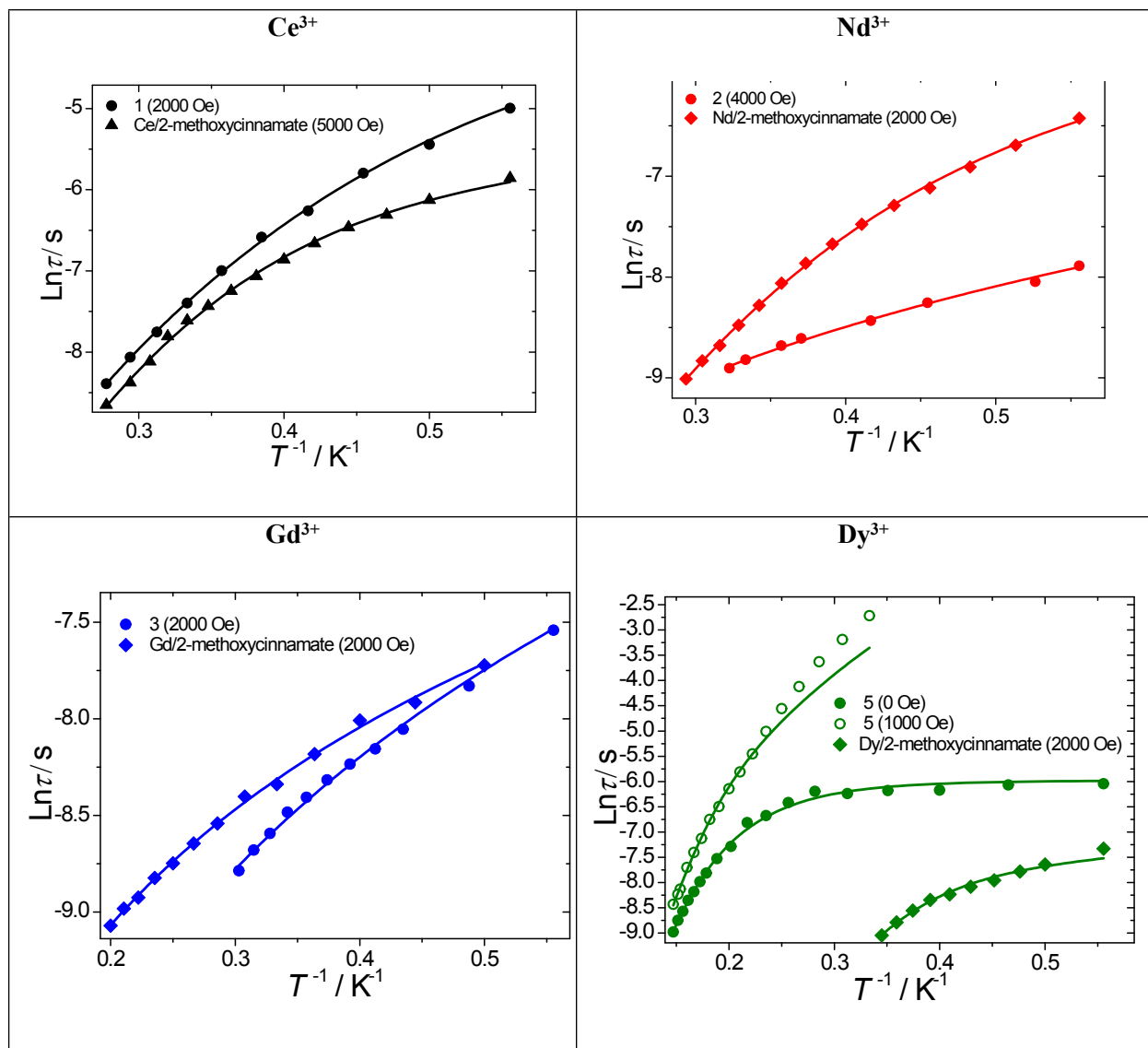


**Figure S15:** Comparison of the temperature dependence of the relaxation time between the dinuclear complexes based on 2-methoxycinnamate ligands.<sup>2</sup>

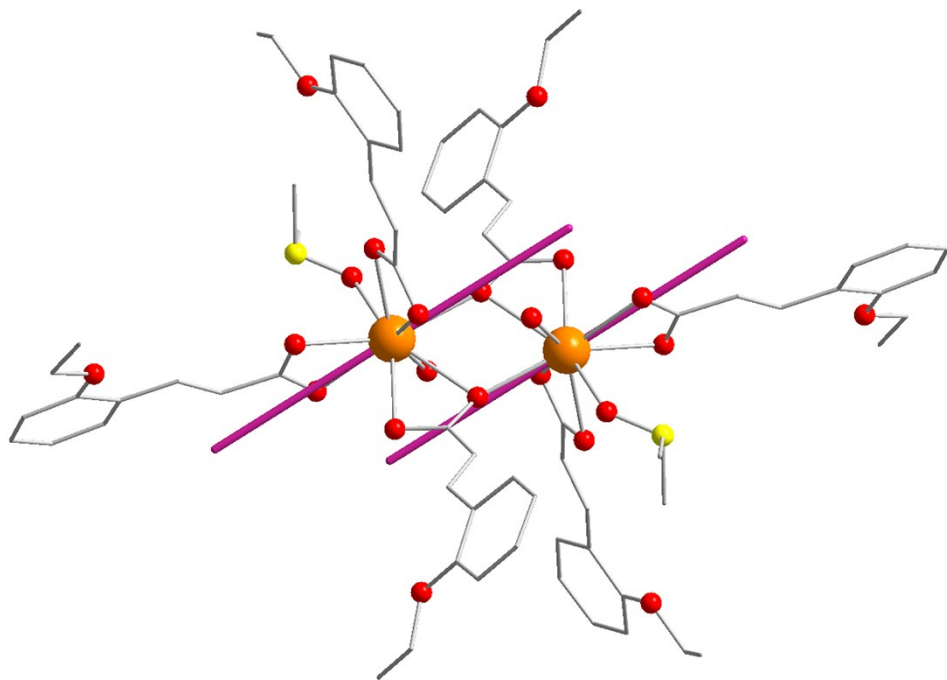


**Figure S16:** Orientation of the anisotropic axes (purple) in **5**.

**Equation used for the fitting of  $\chi T$  vs.  $T$  for 3:**

$$\chi_m T = \frac{2N_g^2 \beta^2}{k} \left[ \frac{e^x + 5e^{3x} + 14e^{6x} + 30e^{10x} + 55e^{15x} + 91e^{21x} + 140e^{28x}}{1 + 3e^x + 5e^{3x} + 7e^{6x} + 9e^{10x} + 11e^{15x} + 13e^{21x} + 15e^{28x}} \right]$$

with  $x = J/kT$

**Table S1:** Crystal data and experimental parameters of structures **1 - 6**.

Complexes reference	1	2	3	4	5	6
<b>Formula</b>	C <sub>35</sub> H <sub>41</sub> CeO <sub>11</sub> S	C <sub>35</sub> H <sub>41</sub> NdO <sub>11</sub> S	C <sub>35.4</sub> H <sub>40.3</sub> GdN <sub>0.3</sub> O <sub>11</sub> S <sub>0.7</sub>	C <sub>36</sub> H <sub>42</sub> TbNO <sub>11</sub>	C <sub>35.7</sub> H <sub>41.7</sub> DyN <sub>0.7</sub> O <sub>11</sub> S <sub>0.3</sub>	C <sub>35.6</sub> H <sub>39.8</sub> ErN <sub>0.6</sub> O <sub>11</sub> S <sub>0.4</sub>
<b>Mass M<sub>w</sub> (g/mol)</b>	809.86	813.98	824.17	823.62	828.81	832.16
<b>Crystal system</b>	Triclinic	Triclinic	Triclinic	Triclinic	Triclinic	Triclinic
<b>Space group</b>	P-1	P-1	P-1	P-1	P-1	P-1
<b>Temperature (K)</b>	200	300	200	200	200	200
<b>a (Å)</b>	8.8932(16)	8.8882(6)	8.544(7)	9.0353(3)	8.3946(2)	8.432(5)
<b>b(Å)</b>	15.015(2)	15.1063(9)	14.813(14)	15.2780(6)	14.6797(4)	14.743(9)
<b>c(Å)</b>	15.167(2)	15.1815(9)	16.466(16)	15.3738(6)	16.3326(5)	16.443(11)
<b>α(°)</b>	65.588(11)	65.367(4)	110.47(3)	60.453(2)	110.372(1)	110.89(2)
<b>γ(°)</b>	87.938(13)	87.895(4)	103.78(2)	74.399(2)	103.423(2)	103.676(16)
<b>β(°)</b>	74.661(13)	74.296(4)	95.51(3)	89.018(2)	95.963(2)	95.403(14)
<b>V(Å<sup>3</sup>)</b>	1772.3(5)	1777.0(2)	1859(3)	1761.24(2)	1797.20(9)	1819.46(2)
<b>Z</b>	2	2	2	2	2	2
<b>dealc. (g.cm<sup>-1</sup>)</b>	1.518	1.521	1.472	1.553	1.532	1.519
<b>μ (mm<sup>-1</sup>)</b>	10.97	12.19	12.35	10.39	11.80	4.99
<b>R<sub>1</sub>[I &gt; 2σ(I)]</b>	0.067	0.041	0.050	0.033	0.033	0.044
<b>wR<sub>2</sub>[I &gt; 2σ(I)]</b>	0.158	0.142	0.128	0.097	0.105	0.123
<b>GOF (F<sup>2</sup>)</b>	0.99	1.09	0.993	1.095	1.047	1.024
<b>Residual electron density, e Å<sup>-3</sup></b> <b>(ρ<sub>min</sub>/ρ<sub>max</sub>)</b>	1.21/-1.35	0.91/-1.02	1.12/-1.03	0.85/-0.75	0.56/-0.74	1.00/-0.94

$$^a R1 = \sum |F_o| - |F_c| / \sum |F_o|; ^b wR2 = \sqrt{\sum [w(F_o^2 - F_c^2)^2] / \sum [w(F_o^2)^2]}$$

**Table S2.** Selected bond distances ( $\text{\AA}$ ) and bond angles ( $^\circ$ ).

	<b>1</b>	<b>2</b>	<b>3</b>	<b>4</b>	<b>5</b>	<b>6</b>
<b>Ln—O1</b>	2.492 (8)	2.478 (6)	2.497 (5)	2.393 (3)	2.457 (3)	2.439 (4)
<b>Ln—O1W</b>	2.557 (9)	2.528 (6)	2.397 (5)	2.428 (3)	2.353 (3)	2.336 (4)
<b>Ln—O2</b>	2.531 (3)	2.515 (6)	2.426 (5)	2.478 (3)	2.391 (3)	2.396 (4)
<b>Ln—O4</b>	2.519 (8)	2.473 (7)	2.471 (5)	2.448 (3)	2.446 (3)	2.434 (4)
<b>Ln—O5</b>	2.540 (9)	2.510 (7)	2.454 (5)	2.442 (3)	2.413 (3)	2.404 (4)
<b>Ln—O7<sup>i</sup></b>	2.562 (8)	2.518 (7)	2.501 (5)	2.483 (3)	2.459 (3)	2.451 (4)
<b>Ln—O8</b>	2.464 (9)	2.434 (6)	2.468 (5)	2.400 (3)	2.405 (3)	2.388 (4)
<b>Ln—O8<sup>i</sup></b>	2.710 (9)	2.680 (7)	2.563 (5)	2.499 (2)	2.529 (3)	2.541 (4)
<b>Ln—O10</b>	2.470 (10)	2.445 (7)	2.410 (5)	2.384 (3)	2.380 (3)	2.363 (4)
<b>O1—Ln—</b>	158.8 (3)	157.6 (2)	128.00 (16)	127.02 (10)	128.15 (10)	128.53 (13)
<b>O1W</b>						
<b>O1—Ln—O4</b>	77.4 (3)	76.7 (2)	74.36 (18)	74.50 (11)	74.42 (11)	74.22 (15)
<b>O1—Ln—O5</b>	102.0 (3)	102.8 (2)	86.06 (16)	79.01 (10)	86.00 (10)	84.81 (14)
<b>O1—Ln—O7<sup>i</sup></b>	76.3 (3)	76.0 (3)	78.95 (19)	71.70 (11)	79.10 (11)	78.80 (15)
<b>O1—Ln—O8<sup>i</sup></b>	107.7 (3)	108.1 (2)	129.11 (17)	113.68 (10)	130.14 (10)	129.83 (15)
<b>O1W—Ln—</b>	90.5 (3)	89.2 (2)	97.2 (2)	78.02 (10)	97.47 (11)	96.32 (15)
<b>O7<sup>i</sup></b>						
<b>O1W—Ln—</b>	74.1 (3)	72.9 (2)	74.96 (17)	75.71 (9)	74.49 (10)	74.18 (13)
<b>O8<sup>i</sup></b>						
<b>O4—Ln—O7<sup>i</sup></b>	153.6 (3)	152.6 (3)	122.82 (18)	136.41 (11)	123.29 (11)	123.93 (14)
<b>O4—Ln—</b>	115.4 (3)	117.6 (2)	138.73 (19)	145.47 (10)	138.02 (11)	138.60 (15)
<b>O1W</b>						
<b>O4—Ln—O8<sup>i</sup></b>	140.1 (3)	139.9 (2)	121.18 (17)	124.08 (9)	121.07 (10)	120.93 (12)
<b>O5—Ln—O8<sup>i</sup></b>	149.9 (3)	148.9 (2)	73.51 (16)	73.27 (9)	73.30 (10)	73.35 (12)
<b>O5—Ln—O7<sup>i</sup></b>	138.2 (3)	138.8 (2)	75.69 (17)	93.32 (10)	75.28 (10)	75.47 (13)
<b>O8—Ln—O1</b>	125.5 (3)	126.8 (2)	153.10 (17)	152.20 (10)	152.55 (11)	152.05 (13)
<b>O8—Ln—O7<sup>i</sup></b>	114.5 (3)	114.5 (2)	115.25 (16)	115.88 (9)	115.81 (10)	116.06 (13)
<b>O8—Ln—O10</b>	153.7 (3)	152.6 (3)	88.71 (18)	78.52 (9)	89.28 (10)	89.25 (14)
<b>O10—Ln—O2</b>	128.86 (3)	129.4 (2)	75.87 (18)	74.49 (10)	75.22 (11)	75.03 (14)
<b>O10—Ln—O8<sup>i</sup></b>	112.4 (3)	113.1 (2)	144.24 (17)	134.48 (10)	144.26 (10)	144.08 (14)

Symmetry transformations used to generate equivalent atoms: Symmetry code: (i) -x, 1-y, 1-z.

**Table S3.** SHAPE analysis.

	JJCU	CCU	JCSAPR	CSAPR	JTCTPR	TCTPR
<b>1</b>	8.035	7.093	4.739	4.115	6.213	4.834
<b>2</b>	8.130	7.237	4.345	3.743	5.952	4.536
<b>3</b>	10.065	8.586	3.192	2.070	3.675	2.784
<b>4</b>	9.835	8.009	3.258	2.453	4.631	2.702
<b>5</b>	9.935	8.504	2.998	1.91	3.476	2.667
<b>6</b>	9.888	8.849	2.929	1.871	3.258	2.514

JJCU: Capped cube

CCU: Spherical-relaxed capped cube

JCSAPR: Capped square antiprism

CSAPR: Spherical capped square antiprism

JTCTPR: Tricapped trigonal prism

TCTPR: Spherical tricapped trigonal prism

**Table S4.** Fitting of the Cole-Cole plots with a sum of two generalized Debye functions for temperature ranging from 1.8 to 6.9 K under a zero dc-field for **5**.

<i>T</i> (K)	$\chi_{S, tot.}$	$\Delta\chi_1$	$\alpha_1$	$\Delta\chi_2$	$\alpha_2$
1.8	3.30295	3.30955	0.1491	7.78267	0.37153
2.15	2.86004	2.83325	0.141	6.4032	0.37573
2.5	0.78189	2.44918	0.13354	7.22443	0.42422
2.85	1.28579	2.20849	0.13831	5.65515	0.41518
3.2	1.73312	1.9988	0.12935	4.39413	0.39736
3.55	1.85616	1.79398	0.10921	3.66252	0.39526
3.9	3.06094	1.43072	0.05957	2.17944	0.38316
4.25	3.22171	1.36357	0.05171	1.52867	0.31532
4.6	3.06674	1.3275	0.05683	1.24661	0.28313
4.95	2.88628	1.28749	0.05687	1.06648	0.24005
5.3	3.03102	1.01216	1.59134E-15	0.84772	0.1686
5.6	2.95678	0.92681	3.18795E-15	0.73082	0.08695
5.8	2.83884	0.90866	2.3744E-15	0.72276	0.08666
6	2.73468	0.80805	2.90533E-15	0.77797	0.10866
6.2	2.67117	0.68537	4.00678E-15	0.82474	0.13549

6.4	2.4146	0.6587	7.45678E-15	0.98125	0.23567
6.6	2.29506	0.67641	8.18393E-15	0.95767	0.20202
6.8	3.30295	3.30955	1.03612E-14	0.94686	0.17624

**Table S5.** Fit parameters of the field dependence of the relaxation time obtained using the Eq. 1

<i>Compound</i>	<i>D</i> ( $s^{-1}K^{-1}Oe^{-4}$ )	<i>B</i> <sub>1</sub> ( $s^{-1}$ )	<i>B</i> <sub>2</sub> ( $Oe^{-2}$ )	<i>K</i>
<b>1</b> (2 K)	$1.16 \times 10^{-1}$	93218	$2.09 \times 10^{-3}$	226.22
<b>5</b> (4 K)	$2.15 \times 10^{-13}$	517.14	$8.38 \times 10^{-5}$	93.9

**Table S6.** Fitting of the Cole-Cole plots with a sum of two generalized Debye functions under a 2000 Oe dc-field for **3**.

<i>T</i> (K)	$\chi_{S\text{tot}}$	$\Delta\chi_1$	$\alpha_1$	$\Delta\chi_2$	$\alpha_2$
1.8	2.55093	3.77723	0.11529	1.25618	0.39325
2.05	2.24909	3.29527	0.13154	1.36141	0.4797
2.3	2.0956	3.01963	0.12599	1.30041	0.50123
2.425	1.99453	3.00598	0.13756	0.94658	0.41612
2.55	1.89493	2.93523	0.13342	1.34498	0.55692
2.675	1.77064	2.87291	0.14387	1.31956	0.5774
2.8	1.74971	2.77603	0.13582	1.28772	0.63695
2.925	1.67364	2.80492	0.15187	0.74517	0.48673
3.05	1.58307	2.74504	0.15917	0.78248	0.56273
3.175	1.52651	2.68258	0.16	0.75889	0.56098
3.3	1.45664	2.69224	0.17718	0.35393	0.31858

**Table S7.** Fitting of the Cole-Cole plots with a generalized Debye model under a 2000 Oe dc-field for **1**.

<i>T</i> (K)	$\alpha$	$\chi_S$ (cm <sup>3</sup> . mol <sup>-1</sup> )	$\chi_T$ (cm <sup>3</sup> . mol <sup>-1</sup> )
--------------	----------	---	---

1.8	0.03361	0.23124	0.20856
2	0.02733	0.20766	0.19079
2.2	0.02253	0.19426	0.14107
2.4	0.02013	0.17298	0.23549
2.6	0.0156	0.16232	0.11335
2.8	0.01021	0.15264	0.1477
3	0.00216	0.14024	0.12795
3.2	2.68102E-15	0.13235	0.12503
3.4	2E-16	0.13061	5.3424E-4
3.6	9.53704E-17	0.12108	0.06149

**Table S8.** Fitting of the Cole-Cole plots with a generalized Debye model under a 4000 Oe dc-field for **2**.

$T$ (K)	$\alpha$	$\chi_s$ (cm <sup>3</sup> . mol <sup>-1</sup> )	$\chi_T$ (cm <sup>3</sup> . mol <sup>-1</sup> )
1.8	0.29702	0.37115	0.93446
1.9	0.26423	0.36816	0.90388
2.1	0.22381	0.33427	0.88996
2.2	0.2294	0.33786	0.88795
2.4	0.18996	0.30506	0.87506
2.5	0.16519	0.29595	0.85939
2.7	0.08931	0.4191	0.50301
2.8	0.07941	0.29146	0.75831
3	0.01865	0.32063	0.61464

**Table S9.** SHAPE analysis comparison between the dysprosium dinuclear complex based on 2-ethoxycinnamate and 2-methoxycinnamate.

JJC <sub>U</sub>	CC <sub>U</sub>	JCSAPR	CSAPR	JTCTPR	TCTPR

<b>5 (2 ethoxycinnamate)</b>	9.935	8.504	2.998	1.91	3.476	2.667
<b>Dy (2-methoxycinnamate)</b>	10.193	8.797	3.103	2.296	3.407	3.058
JJCU: Capped cube						
CCU: Spherical-relaxed capped cube						
JCSAPR: Capped square antiprism						
CSAPR: Spherical capped square antiprism						
JTCTPR: Tricapped trigonal prism						
TCTPR: Spherical tricapped trigonal prism						

1 Y.-N. Guo, G.-F. Xu, Y. Guo and J. Tang, *Dalton Trans.*, 2011, **40**, 9953-9963.

2 O. Khalfaoui, A. Beghidja, J. Long, A. Boussadia, C. Beghidja, Y. Guari and J. Larionova, *Dalton Trans.*, 2017, **46**, 3943-3952.